JOURNAL OF MATERIALS SCIENCE **33** (1998) 5643–5652

Creep behavior in an Al-Fe-V-Si alloy and SiC whisker-reinforced Al-Fe-V-Si composite

L. M. PENG, S. J. ZHU*, F. G. WANG, H. R. CHEN
Department of Materials Engineering, Dalian University of Technology, Dalian 116023, P.R. China
E-mail: zhu@mce.uec.ac.jp

Z. Y. MA, J. BI
Institute of Metal Research, Chinese Academy of Science, Shenyang 110015, P.R. China

High temperature strengthening mechanisms in discontinuous metal matrix composites were examined by performing a close comparison between the creep behavior of 15 vol. pct SiCw/8009Al and that of its matrix alloy, 8009Al. Both the alloy and composite exhibit a single-slope behavior with anomalously high values of apparent stress exponent and high apparent activation energy. The presence of SiC whiskers does not remarkably influence these two kinds of dependence of creep rates but reduces the creep rates by about two orders of magnitude. Transmission electron microscopy examination of the deformation microstructure reveals the occurrence of attractive dislocation/particle interaction. The creep data were analyzed by the threshold stress approach and by the dislocation-climb theories based on attractive interaction between dislocations and dispersoids. All data can be rationalized by a power-law with a stress exponent of 5 and a creep activation energy close to that for the self-diffusion in aluminum. The threshold stress decreases linearly with increasing temperature. General climb together with the attractive but not strong interactions between the dislocations and dispersoids is suggested to be the operative deformation mechanism. The contribution of SiC whiskers to the creep strength of 8009 Al composite can be evaluated quantitatively when the shear-lag model is applied. However, the effects of whisker length and whisker orientation distributions must be considered. Two probability density functions are used for modelling the distribution of whisker length and whisker orientation.

1. Introduction

The development of powder metallurgy technology in the past decade has led to a new family of dispersion-strengthened (DS) Al alloys based on Al-Fe-V-Si system. They maintain their strength at higher temperatures than the other Al-Fe-X systems. The excellent elevated temperature mechanical properties of Al-Fe-V-Si alloys are attributed to the high volume fractions of the ultrafine cubic silicide intermetallic phase, $Al_{12}(Fe,V)_3S$ and its low coarsening rate [1–7].

The superior elevated temperature strength of Al-Fe-X systems has motivated a great deal of study of their creep behavior [2–4, 6–10]. These materials are characterized by high apparent stress exponents and high apparent activation energies for creep, which are similar to the common features of oxide dispersion strengthened (ODS) alloys [11, 12]. Sherby *et al.* [13, 14] have proposed a substructure invariant model which gives the relation

$$\dot{\varepsilon} = A\left(\frac{\lambda}{b}\right)^3\left(\frac{D_L}{b^2}\right)\left(\frac{\sigma}{E}\right)^8 \qquad (1)$$

to describe the creep behavior of such materials. Here $\dot{\varepsilon}$ is the creep rate, λ the subgrain size or the effective dislocation barrier distance, b the Burgers vector, D_L the lattice self-diffusivity, E the elastic modulus, σ the applied stress, and A a dimensionless constant.

Although fine dispersoids can markedly increase the high temperature strength of aluminum alloys, the elastic modulus of these alloys is not significantly increased. The addition of ceramic whiskers or particulates to advanced aluminum alloys can increase the elastic modulus and also creep resistance. Similar to DS alloys, SiC or Al_2O_3 whisker or particulate-reinforced Al composites also involve an abnormally high stress dependence and high activation energy for creep rates [15–23]. However, TiC_p and TiB_{2w} reinforced Ti-6Al-4V composites [24, 25], and SiCw reinforced 6061 Al composites [26] exhibit the same stress exponents and activation energies for creep as the matrix alloy. This implies that the effects of ceramic phases on creep behavior may be matrix-dependent. Therefore, the creep mechanism of discontinuously reinforced aluminum matrix composites needs to be further

* Author to whom all correspondence should be addressed.

studied particularly when the matrix is a dispersion-strengthened alloy [26].

The present article deals with the creep behavior of Al-Fe-V-Si alloy and SiC whiskers reinforced Al-Fe-V-Si composite in the temperature range 573 to 723 K. The dislocation structures and distribution of whiskers and dispersoids were examined by TEM. The creep data were analyzed by the threshold stress approach, by the dislocation-climb theories based on attractive interaction between dislocations and dispersoids and by the modified shear-lag model to examine the effects of dispersoids and whiskers on creep behavior, respectively.

2. Experimental

The atomized Al-8.5Fe-1.3V-1.7Si (by wt %, namely 8009 Al) powders (200 mesh) were produced by Powder Metallurgy Research Institute, Central-South University of Technology, P.R. China. The SiC whiskers, with a diameter of 0.1–0.5 μm and a mean length of 30 μm, were produced by Tokai Co. Ltd., Japan. To obtain good bonding between the whiskers and the matrix, the mixed powders (the volume fraction of SiC whiskers is 0.15) were hot pressed in vacuum at 873 K. The hot pressed billets were then extruded at 733 K with an extrusion ratio of 20:1 [27, 28].

Cylindrical compression test specimens were machined to the following dimensions: 8 mm diameter and 16 mm length, with the compression axis parallel to the extrusion direction. Constant load compression creep tests were performed in air using an electromechanical Mayes ESM 100 testing machine in the temperature range of 573 to 723 K. The test temperature fluctuations were less than ± 1 K. The creep strain was measured by means of a linear variable differential transducer (LVDT). Most creep strain rates were obtained from stress increment tests where the samples were deformed with about 2% strain at which they reached a steady-state stage and then the applied stress was increased. Some compression tests for TEM observation were conducted at a fixed stress and then interrupted when the creep strain was about 3%. After testing, the specimens were cooled under load to preserve the microstructure.

Longitudinal and transverse sections were cut from the specimens and mechanically ground to a thickness of about 60 μm. Thin foils for TEM were then thinned by ion mill at 5 kV and 12°. TEM investigations were performed in JEOL 200 CX microscopy operated at 100 kV.

3. Results

Correlation of the steady-state creep rate of the alloy and composite with the applied stress by a simple power function is plotted in Fig. 1. Apparently, the data points are characterized by a single-slope behavior at the respective testing temperatures and the narrow applied stress range. The values of the apparent stress exponents, $n_a (= \partial \ln \dot{\varepsilon} / \partial \ln \sigma)$, for the creep of 8009 Al and SiCw/8009 Al are both between 14 and 18. Fig. 2 shows the temperature dependence of the steady-state creep

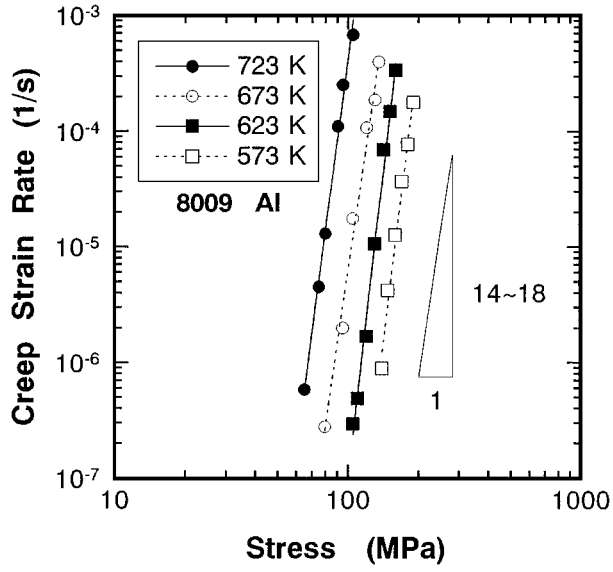

(a)

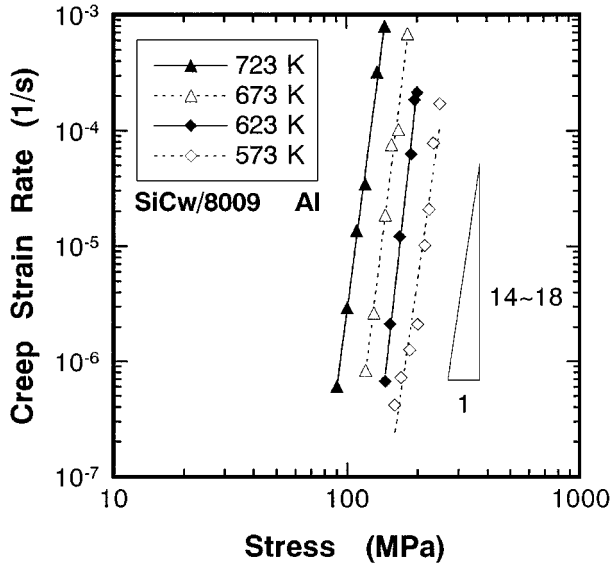

(b)

Figure 1 Variation of steady state creep rate, $\dot{\varepsilon}$ with applied stress, σ at various temperatures ranging from 573 to 723 K. (a) 8009 Al and (b) SiCw/8009 Al.

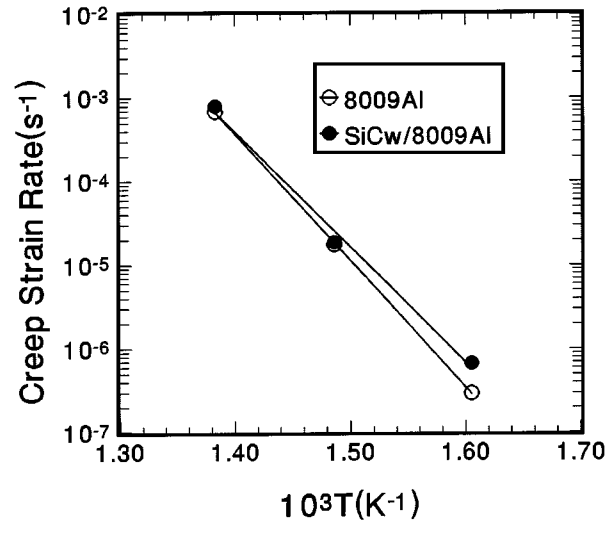

Figure 2 Arrhenius plots of steady state creep rate, $\dot{\varepsilon}$ vs. $10^3/T$ for the data of 8009 Al and SiCw/8009 Al to obtain the apparent activation energy for creep.

rate at constant applied stress. From the slope of the straight lines, a respective creep activation energy of 296 (at 105 MPa) and 273 kJ/mol (at 146 MPa) for 8009 Al and for SiCw/8009 Al is obtained.

It can be found that both the alloy and composite exhibit high stress exponents and high apparent activation energies for creep. These values are much larger than those for creep in pure aluminum or traditional solid solution aluminum alloys (where $n = 3$–5 and $Q_L = 142$ kJ/mol). Moreover, the addition of SiC whiskers does not remarkably influence either the stress or temperature dependence of the creep rates of 8009 Al. This is different from the effects of SiC whiskers or particulates on the creep behavior of pure aluminum or traditional aluminum alloy matrix composites [15–23]. However, it is consistent with the results on the creep of SiC whiskers reinforced 6061 Al composites, in which the matrix contains dispersoids introduced by the powder metallurgy processing [26].

The distribution of dispersoids and whiskers in 8009 Al alloy and its composite is shown in Fig. 3a and b. It can be found that the dispersoids and whiskers are aligned along the extrusion direction. The aspect ratio of SiC whiskers is reduced to about 10 by processing. Dispersoids in as-extruded 8009 Al and dislocation structures after creep test at 673 K and 90 MPa are shown in Fig. 4a and b, respectively. The composition of the dispersoids is close to $Al_{12}(Fe,V)_3Si$ and there are no Al_2O_3 particles detected using selected area diffraction (SAD) through TEM or X-ray diffraction probably due to its too low content [29]. Dislocation/particle interactions are frequently observed in dispersoid-sparse regions. In general, it is difficult to detect such interactions, which may simply be due to the fact that there are relatively much silicide intermetallic particles randomly located through the matrix.

4. Discussion

Considering that the present materials have fine grains and their growth at high temperature is constrained by stable dispersoids and whiskers, constant structure creep equation may be appropriate to explain the present results. Fig. 5 shows that $\dot{\varepsilon}/D_L$ as a function of σ/G follows a narrow data band of each material but the stress exponents are still abnormally high ($n = 14$), where D_L (m^2s^{-1}) $= 1.71 \times 10^{-4} \exp(-142.12/RT)$ [30] and G (MPa) $= 3.0 \times 10^4 - 16T$ [31] (R is the universal gas constant and T is absolute temperature (K)) for pure Al were used. The narrow data band at different temperatures implies that creep rates of the materials may be controlled by lattice diffusion of aluminum. Moreover, it can be found that the addition of SiC whiskers to 8009 Al decreases creep rate by about two orders of magnitude. However, the high stress exponents of the materials are inconsistent with Equation 1.

4.1. Analysis by the threshold stress approach

Creep studies [8, 10, 32, 33] on various RSP Al alloys with submicron-sized grain and discontinuous pure aluminum or aluminum alloy matrix composites [19, 22] have tended to analyze the behavior by incorporating a threshold stress (σ_{th}) into the semi-empirical power-law equation [34]

$$\dot{\varepsilon} = B\frac{D_L G b}{k_B T}\left(\frac{\sigma - \sigma_{th}}{G}\right)^n, \tag{2}$$

where k_B is Boltzmann's constant, G the shear modulus, σ_{th} the threshold stress, B a dimensionless constant, n the true stress exponent and other symbols have been defined previously.

The present experimental data are also examined with such a method. A standard procedure in determining the magnitude of the threshold stress for creep is to plot, on linear coordinates, $\dot{\varepsilon}^{1/n}$ vs. σ and extrapolate the data linearly to zero creep rate [35]. Generally, three values of n of 3, 5, or 8 are selected to construct plots, representing creep by viscous glide [36, 37], high temperature dislocation climb controlled by lattice self-diffusion [38], and the substructure-invariant model of creep [39], respectively. The most appropriate value for n is determined by making several plots of the data on linear coordinates as $\dot{\varepsilon}^{1/n}$ vs. σ using different values of n and then selecting the value of n giving the best linear fit to the datum points. Here we choose the value $n = 5$ because the linear relative coefficients of $\dot{\varepsilon}^{1/n}$ vs. σ curves, R for $n = 5$ are higher than those for $n = 3$ and $n = 8$ [40]. Moreover, the creep behavior of dispersion strengthened Al-Zr-V [8], PM (powder metallurgy) Al_2O_3-2124Al [24] and Al_2O_3-MgO-2124A [41] alloys and discontinuous pure aluminum or aluminum alloy matrix composites [42] is characterized by the true stress exponent, $n = 5$ when the threshold stress approach is used.

Fig. 6 shows the relation of $\dot{\varepsilon}^{1/5}$ as a function of the applied stress. The values of σ_{th} are estimated from the extrapolation of the straight lines and given in Table I. For comparison, the corresponding values of the Orowan stress, σ_{Or} are also listed in this table. The Orowan stress is calculated from the following expression [43]

$$\sigma_{Or} = \frac{0.84\,MGb}{\pi(l - 2r)(1 - \nu)^{1/2}} \ln\left(\frac{r}{b}\right), \tag{3}$$

where M is Taylor factor, r the average particle radius, ν Poisson's ratio, and l the mean particle spacing calculated by [44]

$$l = r\sqrt{\frac{2\pi}{3f_v}}. \tag{4}$$

Here f_v is the volume fraction of particles. For 8009 Al, $M = 3.6$ [45], $\nu = 0.34$ [46], $b = 0.286$ nm, $r = 47$ nm, $f_v = 0.27$ and Equation 4 gives $l = 131$ nm. These structural parameters are assumed to keep constant during creep test since the coarsening rate of dispersoids, $Al_{12}(Fe,V)_3Si$ is quite low and the time for high temperature exposure is not long, i.e. several hours.

In the present study, all the applied stresses are well below the Orowan stress. It is well known that at high

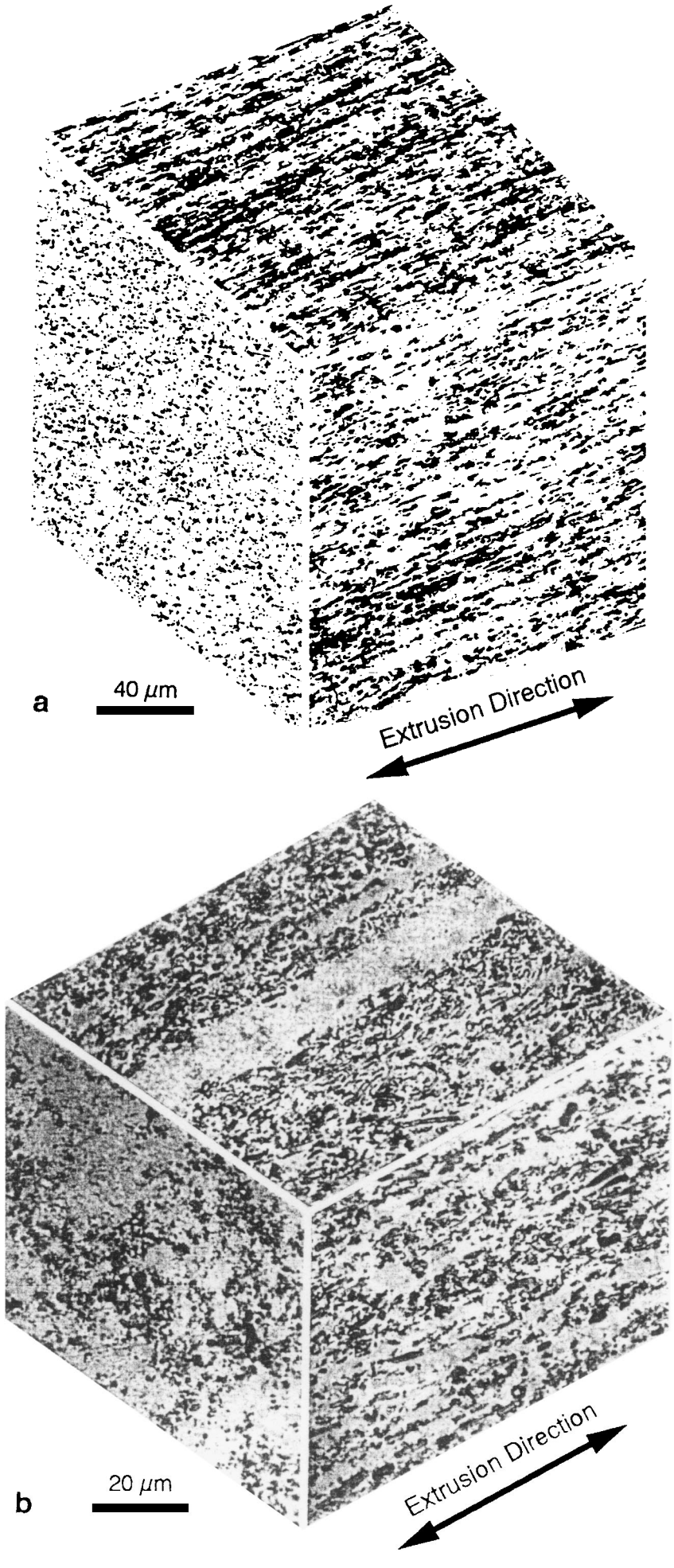

Figure 3 Three-dimensional micrographs of as-extruded (a) 8009 Al and (b) SiCw/8009 Al.

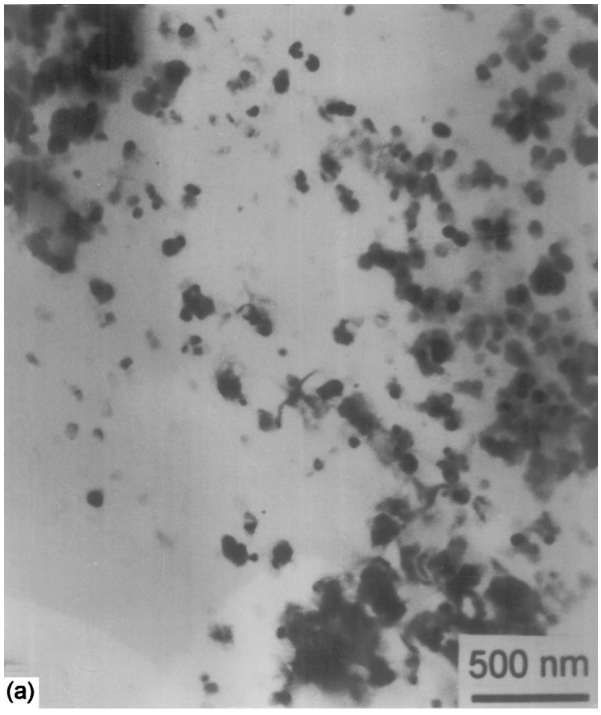

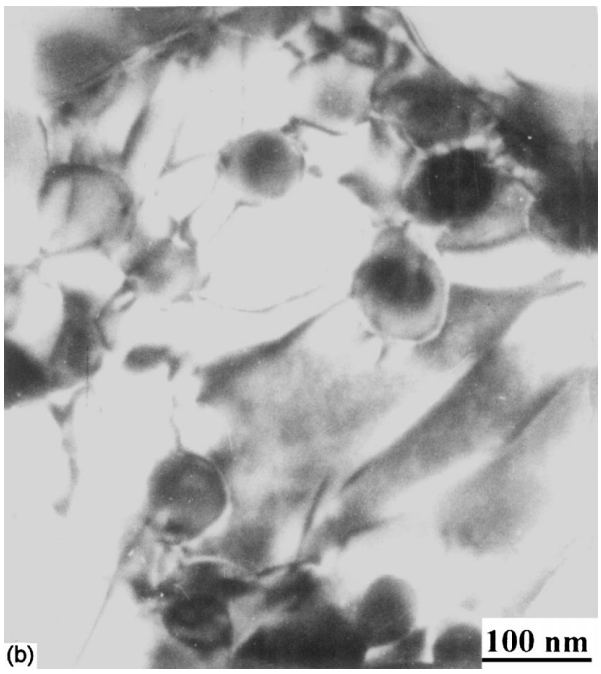

Figure 4 (a) Bright-field transmission electron micrograph of as-extruded 8009 Al showing nearly uniform distribution of dispersoids in the matrix; (b) Dislocation structure in 8009 Al specimen crept at 673 K and 90 MPa.

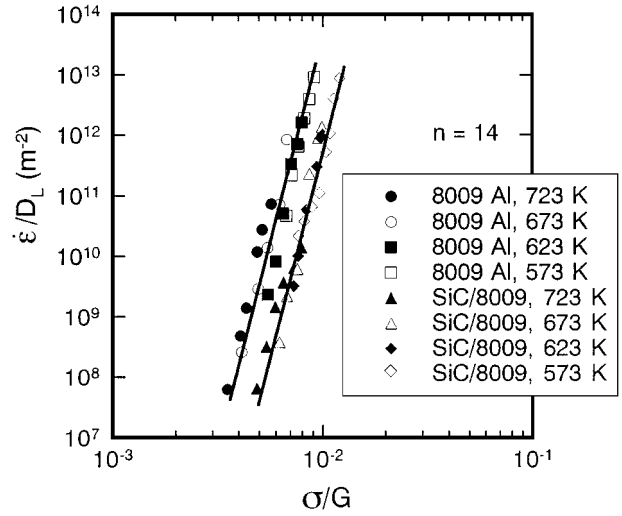

Figure 5 Compression creep strain rates normalized with the lattice diffusion coefficient of aluminum, $\dot{\varepsilon}/D_L$ as a function of the stress compensated with the shear modulus of aluminum, σ/G.

temperatures and below the Orowan stress, dislocations tend to surmount particles by climb mechanism. The models based on local climb, which postulate that the climbing dislocation segment profiles the dispersoids, and the dislocation between the dispersoids remains in its glide plane, lead to a threshold stress between 0.4 and 0.7 σ_{Or} [47, 48]. By contrast, models based on general climb, in which the dislocation is allowed to unravel, lead to a threshold stress between 0.04 and 0.08 σ_{Or} [49, 50]. The ratio of $\sigma_{\mathrm{th}}/\sigma_{\mathrm{Or}}$ observed in this study falls within the latter range, indicating that the dislocation bypass over the dispersoids through the general climb mechanism acts as the predominant deformation mode. However, TEM examination have revealed that there exists an attractive interaction between the dislocations and particles in the 8009 alloy after deformed.

As evident from Table I, the experimental values of the threshold stress, σ_{th} are sensitive to temperature and such a sensitivity cannot be accounted for by the effect of temperature on the shear modulus because the ratio of σ_{th}/G is still temperature-dependent. Mohamed *et al.* [16, 18, 26, 42] analyzed the data of various reinforced and superplastic alloys by means of a threshold stress with a temperature dependence given by

$$\frac{\sigma_{\mathrm{th}}}{G} = B \exp\left(\frac{Q_{\mathrm{th}}}{RT}\right), \tag{5}$$

TABLE I Values of threshold stress determined from Equation 2 and Orowan stress from Equation 3

		8009Al			SiCw/8009 Al		
T (K)	σ_{Or} (MPa)	σ_{th}	$\sigma_{\mathrm{th/G}}$	$\sigma_{\mathrm{th}}/\sigma_{\mathrm{Or}}$	σ_{th}	σ_{th}/G	$\sigma_{\mathrm{th}}/\sigma_{\mathrm{Or}}$
573	973	112	5.38E−3	0.115	132	6.34E−3	0.136
623	935	95	4.74E−3	0.102	123	6.14E−3	0.132
673	898	70	3.64E−3	0.078	101	5.26E−3	0.112
723	861	55	2.98E−3	0.064	78	4.23E−3	0.091

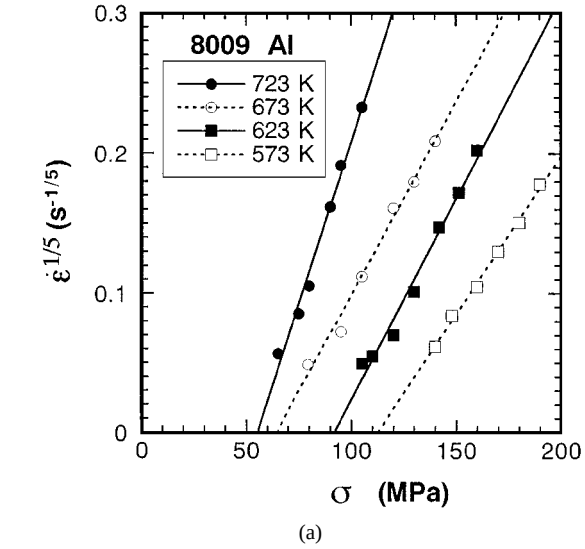

(a)

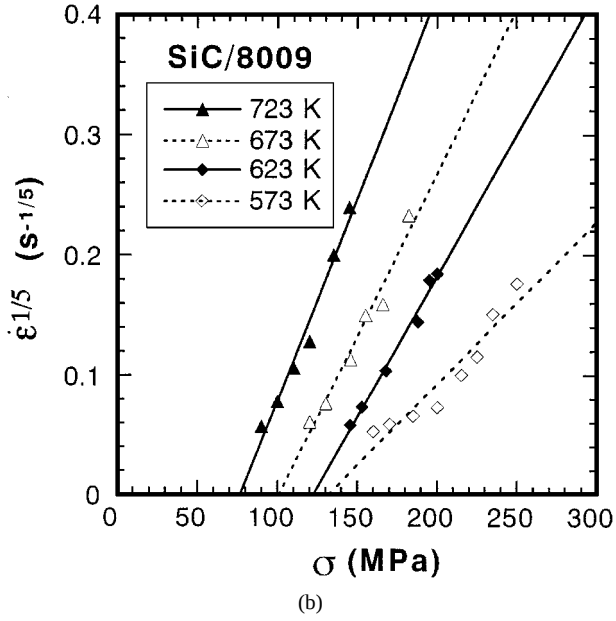

(b)

Figure 6 Variation of $\dot{\varepsilon}^{1/5}$ with stress, σ on double linear scales and extrapolating the curves to obtain the threshold stresses, σ_{th} at various temperatures. (a) 8009 Al and (b) SiCw/8009 Al.

where B is a constant and Q_{th} has the meaning of an activation energy for the threshold stress, which may be a reflection of an interaction between impurities that are able to segregate at incoherent particles and dislocations that are captured at the detachment side of the particles [51]. Then, the relation between apparent activation energy, Q_a and self-diffusion energy, Q_L can be expressed as follows

$$Q_a = Q_L - \frac{nRT^2}{G}\cdot\frac{\partial G}{\partial T}\left(1+\frac{1}{\sigma/\sigma_{\text{th}}-1}\right)-\frac{nQ_{\text{th}}}{\sigma/\sigma_{\text{th}}-1}. \tag{6}$$

However, the calculated values of Q_a will become unreasonably large when the applied stress approaches the threshold stress [40].

Mishra *et al*. [52] use a dependence of the threshold stress with the temperature given by

$$\sigma_{\text{th}} = -C + \frac{C'}{T}, \tag{7}$$

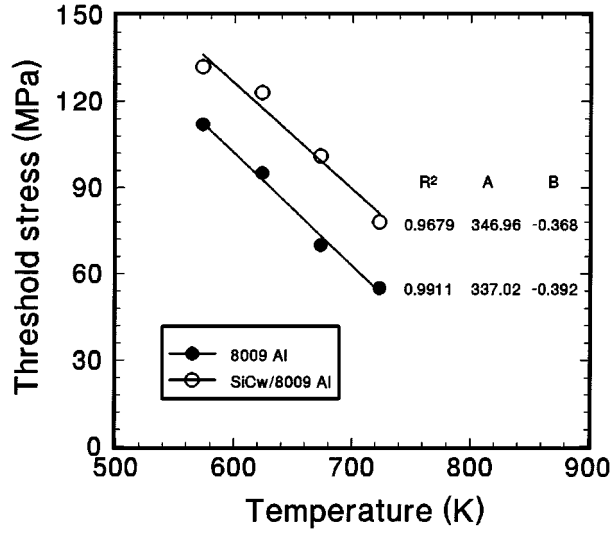

Figure 7 The threshold stress σ_{th} plotted against the absolute testing temperature, T in the interval 573–723 K (R is the relative coefficient).

where C and C' are constants. This dependence of σ_{th} with temperature is much too weak to describe the creep behavior of our materials. Furthermore, these authors attributed such temperature dependence to a change in Young's modulus with temperature which is far from true in our materials as shown in Table I.

Here, we adopt the following equation [21] to describe the temperature dependence of threshold stress as shown in Fig. 7

$$\frac{\sigma_{\text{th}}}{G} = \left(\frac{\sigma_{\text{th}}}{G}\right)_{T=0}\left(1-\frac{T}{T_c}\right) = A + BT, \tag{8}$$

where $(\sigma_{\text{th}}/G)_{T=0}$ is the normalized threshold stress at absolute temperature, T approaching zero K, T_c is the critical temperature when (σ_{th}/G) is equal to zero, A and B are constants.

Then, using the procedure described by Cadek *et al.* [22] the expression

$$Q_a = Q_L - \frac{nRT^2}{G}\left[\frac{n-1}{n}\cdot\frac{\partial G}{\partial T}+\frac{G}{\sigma-\sigma_{\text{th}}}\cdot\frac{\partial\sigma_{\text{th}}}{\partial T}\right] \tag{9}$$

is obtained for the apparent activation energy of creep Q_a, where Q_L is the activation energy for lattice self-diffusion in pure aluminum. From Equation 9 it follows that Q_a depends not only on applied stress but also on temperature, since the threshold stress σ_{th} depends on temperature: $\mathrm{d}\sigma_{\text{th}}/\mathrm{d}T = B = -0.392$ (MPa K^{-1}) for 8009 Al and $\mathrm{d}\sigma_{\text{th}}/\mathrm{d}T = B = -0.368$ (MPa K^{-1}) for SiCw/8009 Al (cf. Fig. 7), respectively. The apparent activation energy Q_a is, in general, significantly higher than that for lattice self-diffusion, Q_L, especially at low applied stress. This was convincingly demonstrated by Cadek *et al.* [19, 22] who compared the values of Q_a obtained analyzing the experimental $\dot{\varepsilon}(T,\sigma)$ relationships for various temperatures and applied stresses with the values of Q_a calculated by means of Equation 9. Only a few examples, (i.e. for a temperature of 723 K and applied stresses of 95, 105 MPa for 8009 Al,

TABLE II Values of the apparent activation energies Q_a^{calc} and Q_a^{exp} for 723 K and applied stress 95, 105 MPa for 8009 Al, 146 MPa for SiCw/8009 Al and unrealistically high stress, i.e. $\sigma = 500$ MPa for these two materials (all terms of energies are in unit of kJ/mol)

	8009 Al		SiCw/8009 Al	
σ (MPa)	Q_a^{calc}	Q_a^{exp}	Q_a^{calc}	Q_a^{exp}
95	367.7	392	—	—
105	325.1	296	—	—
146	—	—	272.3	273
500	173.9	—	173.7	—

146 MPa for SiCw/8009 Al and 500 MPa) for these two materials will be given here. The value of Q_a obtained from experimentally determined $\dot{\varepsilon}(T, \sigma)$ relationship will be denoted Q_a^{exp} and its value, calculated by means of equation (3), Q_a^{calc}, respectively. The results are presented in Table II, from which it can be seen that the values of Q_a^{exp} are in reasonable agreement with those of Q_a^{calc}. At the same time, Q_a^{exp} and Q_a^{calc} are significantly higher than Q_L. It is worth mentioning that even for the same temperature of 723 K but for an unrealistically high applied stress, i.e. $\sigma = 500$ MPa, the values of Q_a^{calc} are still noticeably higher than the value of Q_L (see Table II). This is in full agreement with Cadek *et al.*'s results for some SiCp/Al composites [19, 22].

Normalizing the creep strain rate to the coefficient of self-diffusion D_L as well as the effective applied stress to the shear modulus G for aluminum and plotting $\dot{\varepsilon}/D_L$ against $(\sigma - \sigma_{th})/G$ in the double logarithmic coordinates as shown in Fig. 8, the creep data at all temperatures in either 8009 Al or the composite can be described by a straight line with a slope of about 5 over more than five orders of magnitude of the normalized

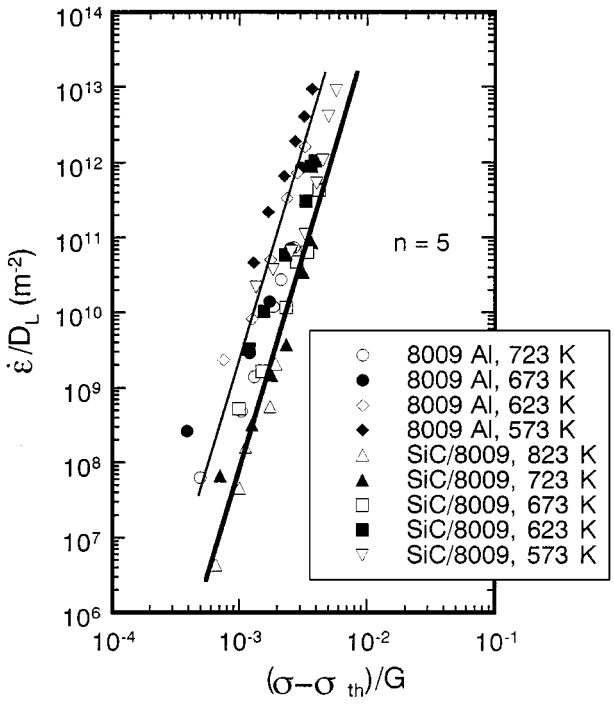

Figure 8 Creep strain rate normalized with the lattice diffusion coefficient of aluminum, $\dot{\varepsilon}/D_L$ as a function of the effective stress compensated with the shear modulus of aluminum, $(\sigma - \sigma_{th})/G$.

creep rates. This implies that the true stress exponent for creep is 5 and the creep rates in both 8009 Al and the composite are controlled by the lattice diffusion in aluminum matrix. However, the normalized creep rates of the SiCw/8009 Al is still lower than those of 8009 Al. The parallel curves between 8009 Al and the composite in Figs 5 and 8 imply that the difference may be caused by a load transfer mechanism.

4.2. Analysis by dislocation detachment mechanism

Recently, Arzt and coworkers [53, 54] have proposed an exponential law based on an attractive interaction between dislocation and particles. Their equation for the creep strain rate is

$$\dot{\varepsilon} = C D_L \exp\left\{-\frac{Gb^2 r}{k_B T}\left[(1-k)\left(1-\frac{\sigma}{\sigma_d}\right)\right]^{3/2}\right\}, \tag{10}$$

where $C = 3l\rho/b$ is the structure-dependent parameter, l the half particle spacing, ρ the mobile dislocation density, k the relaxation parameter, defined as the ratio of the dislocation line tension of the particle/matrix interface to the line tension in the matrix remote from the particle, σ_d the athermal detachment stress given by the expression

$$\sigma_d = \sigma_{Or}\sqrt{1-k^2}. \tag{11}$$

The ratio of the applied stress to the detachment stress, σ/σ_d, is calculated using the expression

$$\frac{\sigma}{\sigma_d} = \left[\frac{3(Q_a - Q_L)}{2RTn_a\left(1 - \frac{\partial G}{\partial T}\frac{T}{G}\right)} + 1\right]^{-1} \tag{12}$$

where n_a is the apparent stress exponent and Q_a the apparent activation energy for creep. Then the interaction parameter k can be obtained by fitting the creep data to the following equation

$$k = 1 - \left(\frac{2k_B T}{3Gb^2 r} \cdot \frac{n_a}{(1-\sigma/\sigma_d)^{1/2} \cdot \sigma/\sigma_d}\right)^{2/3}. \tag{13}$$

The estimated values of the detachment stress, σ/σ_d and the interaction parameter k for 8009 Al at the respective temperatures are listed in Table III.

High values of the interaction parameter indicate that there exists a weaker attractive interaction between

TABLE III Calculation of the detachment stress, σ/σ_d and the interaction parameter k at the respective temperatures

T (K)	G (GPa)	n_a	σ/σ_d	k
573	20.83	17	0.325	0.974
623	20.03	18	0.365	0.972
673	19.23	14	0.337	0.973
723	18.43	16	0.390	0.971

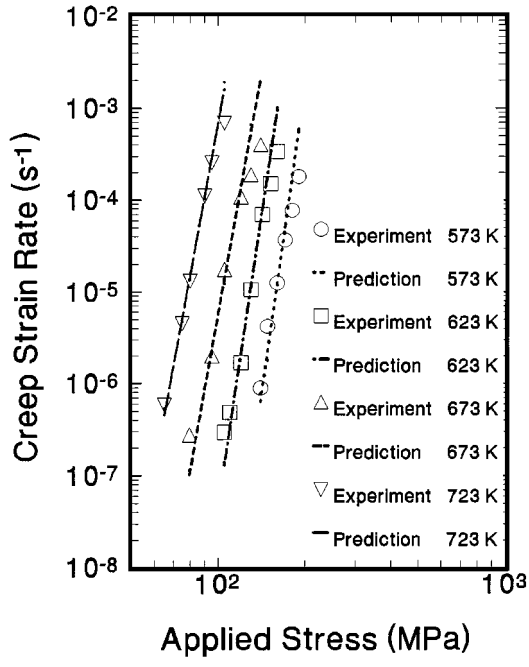

Figure 9 Variation of creep strain rate with stress for 8009 Al. The curves represent prediction at different temperatures using detachment controlled dislocation model. A good correlation between experimental data (points) and theoretical results (curves) is observed.

the dislocations and particles. According to Arzt and Wilkinson, the critical value of k below which dislocation bypass becomes detachment controlled is 0.94. However, this transition would be shifted to higher values when the climb process was "general" instead of "local" [55].

The results of the preceding analysis were used to predict the stress dependence of the creep rate over the range of the test temperatures. The creep rate at different temperatures was evaluated using the values of k and σ_d in Equation 10 and plotted as $\dot{\varepsilon}$ vs. σ in Fig. 9. It is apparent that the model provides an acceptable description of the data.

From the above analysis, general climb together with the attractive but not strong interactions between dislocations and particles is suggested to be the operative deformation mechanism. The weak attractive interactions between dislocations and particles make the dislocation general climb a dominant mechanism. This mechanism accounts for the threshold stress and the observed single-slope behavior in the relationship between the stress and creep rate.

4.3. The effect of SiC whisker on creep behavior of 8009 Al

Kelly *et al.* [56, 57] have proposed a simple continuum mechanics model to predict the creep behavior of discontinuously fiber reinforced composites. Based on the assumption that the stress exponent for the composite is equal to that for the matrix alloy and that there is no interfacial debonding, the original analysis of Kelly leads to the following expression to predict the composite creep rate

$$\dot{\varepsilon}_c = \dot{\varepsilon}_m \left[\beta \left(\frac{L}{d} \right)^{\frac{n+1}{n}} V_f + (1 - V_f) \right]^{-n}, \qquad (14)$$

where $\dot{\varepsilon}_c$ is the composite creep rate, $\dot{\varepsilon}_m$ the matrix creep rate at the same temperature and stress, L/d the aspect ratio of the reinforcement, V_f the volume fraction of the reinforcement, n the matrix stress exponent, and β the load transfer coefficient determined by

$$\beta = \left(\frac{2}{3} \right)^{\frac{1}{n}} \left(\frac{n}{2n+1} \right) \left[\left(\frac{2\sqrt{3}}{\pi} V_f \right)^{-\frac{1}{2}} - 1 \right]^{-\frac{1}{n}}. \qquad (15)$$

For the present SiCw/8009 Al composite, using $n = 14$, $V_f = 0.15$, and $L/d = 10$, Equation 15 gives the value of β as 0.456. Then the ratio of $\dot{\varepsilon}_c/\dot{\varepsilon}_m$ as 8.55×10^{-4} is obtained from Equation 14. This value demonstrates that the addition of SiC whiskers decreases creep rate by about three orders of magnitude. However, it can be found from Figs 5 and 8 that the theoretical prediction based on the shear-lag model underestimates the composite creep rate by nearly one order of magnitude.

During extrusion process, progressive and continuous changes in whisker orientation occurs, and whiskers are misaligned. Moreover, some whiskers will inevitably be broken in a whisker length distribution with an asymmetric character. Therefore, the assumptions in the shear-lag model are not consistent with the real case and some modifications must be made. Here, χ_1 and χ_2 are introduced to represent the whisker orientation and whisker length factors, respectively, and $\chi_1\chi_2$, is the whisker efficiency factor for the strengthening of the composite: the larger the value of $\chi_1\chi_2$, the higher the composite strength. Then Equation 14 can be modified as follows:

$$\dot{\varepsilon}_c = \dot{\varepsilon}_m \left[\chi_1\chi_2\beta \left(\frac{L}{d} \right)^{\frac{n+1}{n}} V_f + (1 - V_f) \right]^{-n}. \qquad (16)$$

If $\theta = 0$ (where θ is the whisker orientation angle), χ_1 should be equal to 1 and it is the case for unidirectionally aligned whisker composite. Then the fibre length factor is [58]

$$\chi_2 = \int_0^{L_c} \left[\frac{L^2}{2L_cL_{\text{mean}}} \right] f(L)\,\mathrm{d}L + \int_{L_c}^{\infty} \left(\frac{L}{L_{\text{mean}}} \right) \left(1 - \frac{L_c}{2L} \right) f(L)\,\mathrm{d}L, \qquad (17)$$

where L_c is the critical whisker length, L_{mean} the mean whisker length and $f(L)$ the two-parameter Weibull distribution function to describe the whisker length distribution and given by [59]

$$f(L) = abL^{b-1}\exp(-aL^b) \quad \text{for} \quad L > 0 \qquad (18)$$

where a and b are scale and shape parameter, respectively.

TABLE IV The effect of whisker orientation distribution on the whisker efficiency factor

No.	p	q	χ_1	$\chi_1\chi_2$
1	0.5	1	0.33	0.228
2	1	4	0.60	0.415
3	1	8	0.78	0.540
4	1	16	0.88	0.609
5	0.5	10	0.91	0.630
6	4	100	0.92	0.637
7	0.5	16	0.94	0.650
8	0.5	32	0.97	0.671
9	1	100	0.98	0.678
10	0.5	100	0.99	0.685

Similarly, Xia *et al*. [60] proposed a two-parameter exponential function to describe the whisker orientation distribution and the function is given as

$$g(\theta) = \frac{(\sin\theta)^{2p-1}(\cos\theta)^{2q-1}}{\int_{\theta_{\min}}^{\theta_{\max}}(\sin\theta)^{2p-1}(\cos\theta)^{2q-1}\,\mathrm{d}\theta}, \qquad (19)$$

where p and q are the shape parameters which can be used to determine the shape of the distribution curve, and $p \geq 1/2$ and $q \geq 1/2$. Also, $0 \leq \theta_{\min} \leq \theta \leq \theta_{\max} \leq \pi/2$. Then the whisker orientation coefficient, χ_1, can be defined as [47]

$$\chi_1 = 2\int_{\theta_{\min}}^{\theta_{\max}} g(\theta)\cos^2(\theta)\,\mathrm{d}\theta - 1. \qquad (20)$$

Table IV gives the effect of whisker orientation distribution on the value of $\chi_1\chi_2$, where $L_{\min} = 0$, $L_{\max} = \infty$, $L_{\mathrm{mean}} = 12.5\,\mu$m, $L_{\mathrm{mod}} = 10\,\mu$m and $L_c = 6\,\mu$m, respectively. The value of χ_1 is calculated according to Equation 20 based on the different values of p and q. Now based on the real whisker orientation distribution in SiCw/8009 Al (see Fig. 3(b)), $\chi_1 = 0.94$ and $\chi_1\chi_2 = 0.650$ are reasonable values for evaluating the effect of SiC whiskers on the creep rates. Incorporation of $\chi_1\chi_2$ into Equation 16 yields the ratio of $\dot{\varepsilon}_c/\dot{\varepsilon}_m = 1.16 \times 10^{-2}$ which means that the addition of SiC whiskers decreases creep rate by about two orders of magnitude. This theoretical result is verified by the experimental data (see Figs 5 and 8).

In addition, a comparison between the creep rates corrected for load transfer for SiCw/8009 Al was conducted by plotting the normalized strain rate, $\dot{\varepsilon}/D_L$ against the normalized effect stress, $(1-\phi)(\sigma-\sigma_{\mathrm{th}})/G$ (where $\phi = \chi_1\chi_2\beta = 0.296$ for the composite and $\phi = 0$ for the alloy, respectively) in Fig. 10. As shown by this figure, the normalized strain rates of the composite are very close to those of the alloy.

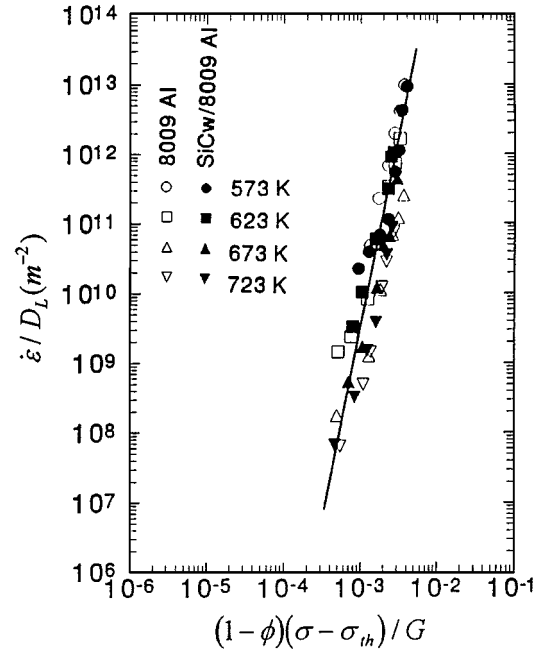

Figure 10 A plot of the normalized strain rate, $\dot{\varepsilon}/D_L$ vs. the normalized effective stress, $(1-\phi)(\sigma-\sigma_{\mathrm{th}})/G$ for 8009 Al and SiCw/8009 Al for $n = 5$. The strain rates of the composite are corrected by considering the effect of load transfer based on the modified Shear-Lag model.

5. Conclusions

(1). Application of the power-law creep equation to the creep data obtained by constant compression load creep tests results in anomalously high apparent stress exponent (up to 18) and activation energies of 296 and 273 kJ/mol for creep behavior of DS 8009 Al and SiCw/8009 Al, respectively. The presence of SiC whiskers does not influence these two kinds of dependence remarkably but reduces the creep rates by about two orders of magnitude.

(2). By considering a threshold stress, all data can be rationalized by a power-law with a stress exponent of 5 and a creep activation energy close to the self-diffusion activation energy of the matrix lattice. The threshold stress is equal to 0.064–0.136 of the Orowan stress and decrease with temperatures.

(3). General climb together with an attractive but not strong interaction between the dislocations and particles is suggested to be the operative deformation mechanism in 8009 Al alloy.

(4). The creep strengthening of SiC whiskers is achieved through two effects, namely increasing threshold stress and sharing a part of applied stress. The latter effect can be described quantitatively by the modified shear-lag model considering the effects of whisker length and whisker orientation distributions which have been characterized by two probability density functions.

Acknowledgements

Financial support from National Natural Science Foundation of China (No. 59471047) is gratefully acknowledged. The authors are deeply indebted to Professor Z. G. Wang for his permission to use the facilities. We are also grateful to Mr. L. Liu, Ms. K. Liu, Mr. G. Yao, and Mr. J. S. Wu for assisting with some parts of the experimental work.

References

1. D. J. SKINNER, R. L. BYE, D. RAYBOULD and A. M. BROWN, *Scripta Metall. Mater.* **20** (1986) 867.

2. G. M. PHARR, M. S. ZEDALIS, D. S. SKINNER and P. S. GILMAN, in "Dispersion Strengthening Aluminum Alloys," edited by Y. W. Kim and W. M. Griffth (TMS, Warrendale, PA, 1988) p. 309.
3. G. S. MURTY and M. J. KOCZAK, *J. Mater. Sci.* **24** (1989) 510.
4. S. C. KHATRI and M. J. KOCZAK, *Mater. Sci. Eng.* **A167** (1993) 11.
5. J. C. EHRSTRÖM and A. PINEAU, *ibid.* **A186** (1994) 55.
6. S. MITRA, *Metall. Trans.* **27A** (1996) 3913.
7. M. A. RODRIGUEZ and D. J. SKINNER, *J. Mater. Sci. Lett.* **9** (1990) 1292.
8. Y. C. CHEN, M. E. FINE and J. R. WEERTMAN, *Acta Metall. Mater.* **38** (1990) 771.
9. D. LEGZDINA and T. A. PARTHASARATHY, *Metall. Trans.* **21A** (1990) 2155.
10. M. K. PREMKUMAR, A. LAWLEY and M. J. KOCZAK, *Mater. Sci. Eng.* **A174** (1994) 127.
11. K. R. WILLIAMS and B. WILSHIRE, *J. Mater. Sci.* **7** (1973) 176.
12. H. BURT, J. P. DENNISON and B. WILSHIRE, *ibid.* **13** (1979) 295.
13. J. LIN and O. D. SHERBY, *Res. Mechanica* **2** (1981) 251.
14. J. WOLFENSTINE, G. GONZALEZ-DONCEL and O. D. SHERBY, *J. Mater. Sci. Lett.* **9** (1990) 410.
15. T. L. DRAGONE and W. D. NIX, *Acta Metall. Mater.* **38** (1990) 1941.
16. K. T. PARK, E. J. LAVERNIA and F. A. MOHAMED, *ibid.* **38** (1990) 2149.
17. T. L. DRAGONE and W. D. NIX, *ibid.* **40** (1992) 2781.
18. F. A. MOHAMED, K. T. PARK and E. J. LAVERNIA, *Mater. Sci. Eng.* **A159** (1992) 21.
19. J. CADEK, H. OIKAWA and V. SUSTEK, *ibid.* **A190** (1995) 9.
20. A. B. PANDEY, R. S. MISHRA and Y. R. MAHAJAN, *Acta Metall. Mater.* **40** (1992) 2045.
21. G. GONZALEZ-DONCEL and O. D. SHERBY, *ibid.* **41** (1993) 2797.
22. J. CADEK, V. SUSTEK and M. PAHUTOVA, *Mater. Sci. Eng.* **A174** (1994) 141.
23. K. T. PARK and F. A. MOHAMED, *Metall. Trans.* **26A** (1995) 3119.
24. S. J. ZHU, Y. X. LU, Z. G. WANG and J. BI, *Mater. Lett.* **13** (1992) 199.
25. S. J. ZHU, Y. X. LU, Z. G. WANG and J. BI, in "Metal Matrix Composites," Vol. I edited by A. Miravete (Woodhead Publishing Limited, Abington, Cambridge, 1993) p. 549.
26. K. T. PARK, E. J. LAVERNIA and F. A. MOHAMED, *Acta Metall. Mater.* **42** (1994) 667.
27. Z. Y. MA, X. G. NING, Y. X. LU, J. H. LI, J. BI and Y. Z. ZHANG, *Mater. Lett.* **21** (1994) 69.
28. Z. Y. MA, J. PAN, X. G. NING, J. H. LI, Y. X. LU and J. BI, *J. Mater. Sci. Lett.* **13** (1994) 1731.
29. S. J. ZHU, L. M. PENG, Z. Y. MA, J. BI, F. G. WANG and Z. G. WANG, *Mater. Sci. Eng.* **A215** (1996) 120.
30. T. S. LUNDY and J. F. MURDOCK, *J. Appl. Phys.* **33** (1962) 1671.
31. J. E. BIRD, A. K. MUKHERJEE and J. E. DORN, in "Quantitative Relations between Properties and Microstructures," edited by D. G. Brandon and A. Rosen (Israel University Press, Jerusalem, 1969) p. 225.
32. M. K. PREMKUMAR, M. J. KOCZAK and A. LAWLEY, in "High Strength Powder Metallurgy Aluminum Alloys," edited by G. Hildemand and M. J. Koczak (The Metallurgical Society, Warrendale, PA, 1986) p. 265.
33. R. S. MISHRA, A. G. PARADLAR and K. N. RAO, *Acta Metall. Mater.* **41** (1993) 2243.
34. J. E. BIRD, A. K. MUKHERJEE and J. E. DORN, *Trans. Amer. Soc. Met.* **62** (1969) 155.
35. R. LAGNEBORG and B. BERGMAN, *Met. Sci.* **10** (1976) 20.
36. J. WEERTMAN, *J. Appl. Phys.* **28** (1957) 1185.
37. F. A. MOHAMED and T. G. LANGDON, *Acta Metall. Mater.* **22** (1974) 779.
38. J. WEERTMAN, *J. Appl. Phys.* **28** (1957) 362.
39. O. D. SHERBY, R. H. KLUNDT and A. K. MILLER, *Metall. Trans.* **8A** (1977) 843.
40. L. M. PENG, Ph.D. dissertation, Dalian University of Technology, Dalian, P.R. China, 1998.
41. L. KLOC, S. SPIGARELLI, E. CERRI, E. EVANGELISTA and T. G. LANGDON, *Acta Metall. Mater.* **45** (1997) 529.
42. Y. LI, S. R. NUTT and F. A. MOHAMED, *ibid.* **45** (1997) 2607.
43. U. F. KOCKS, *Phil. Mag.* **13A** (1966) 541.
44. J. RÖSLER, R. JOOS and E. ARZT, *Metall. Trans.* **23A** (1992) 1521.
45. W. KOSTER and H. FRANZ, *Met. Rew.* **6** (1961) 1.
46. G. LEROY, J. D. EMBURY, E. EDWARD and M. F. ASHBY, *Acta Metall. Mater.* **29** (1981) 1509.
47. L. M. BROWN and R. K. HAM, in "Strengthening Methods in Crystals," edited by A. Kelly and R. B. Nicolson (Elsevier, Amsterdam, 1971) p. 9.
48. R. S. W. SHEWFELT and L. M. BROWN, *Phil. Mag.* **35A** (1977) 945.
49. R. LAGNEBORG, *Scripta Metall. Mater.* **7** (1973) 605.
50. J. H. HAUSSELT and W. D. NIX, *Acta Metall. Mater.* **25** (1977) 1491.
51. J. FRIEDEL, Dislocation (Addison-Wesley, Oxford, 1982) Chap. 16.
52. R. S. MISHRA and A. B. PANDEY, *Metall. Trans.* **21A** (1990) 2089.
53. J. RÖSLER and E. ARZT, *Acta Metall. Mater.* **38** (1990) 671.
54. E. ARZT, *Res. Mechanica* **31** (1991) 399.
55. E. ARZT and D. S. WILKINSON, *Acta Metall. Mater.* **34** (1986) 1893.
56. A. KELLY and K. N. STREET, *Proc. Roy. Soc. London* **328A** (1972) 267.
57. *idem.*, *ibid.* **328A** (1972) 283.
58. S. Y. FU and B. LAUKE, *Comp. Sci. Tech.* **52** (1996) 1179.
59. F. ULRYCH, M. SOVA, J. VOKROUHLECKY and B. TURCIC, *Polym. Comp.* **14** (1993) 229.
60. M. XIA, H. HAMADA and Z. MAEKAWA, *Int. Polym. Process.* **5** (1995) 74.

Received 29 October 1997
and accepted 15 September 1998